# The compressibility of cubic white and orthorhombic, rhombohedral, and simple cubic black phosphorus

S. M. Clark[1,2] and J. M. Zaug[3]

[1]Advanced Light Source, Lawrence Berkeley National Laboratory, 1 Cyclotron Road, Berkeley CA 94720, USA.

[2]Department of Earth and Planetary Sciences, University of California, Berkeley, CA 94720, USA.

[3]Physical & Life Sciences, Lawrence Livermore National Laboratory, 7000 E. Avenue, L-350, Livermore CA, 94551, USA.

The effect of pressure on the crystal structure of white phosphorus has been studied up to 22.4 GPa. The α phase was found to transform into the α' phase at 0.87 ± 0.04 GPa with a volume change of 0.1 ± 0.3 cc/mol. A fit of a second order Birch-Murnaghan equation to the data gave Vo = 16.94 ± 0.08 cc/mol and $K_o$ = 6.7 ± 0.5 GPa for the α phase and Vo = 16.4 ± 0.1 cc/mol and $K_o$ = 9.1 ± 0.3 GPa for the α' phase. The α' phase was found to transform to the A17 phase of black phosphorus at 2.68 ± 0.34 GPa and then with increasing pressure to the A7 and then simple cubic phase of black phosphorus. A fit of a second order Birch-Murnaghan equation to our data combined with previous measurements gave Vo = 11.43 ± 0.05 cc/mol and $K_o$ =

34.7 ± 0.5 GPa for the A17 phase, Vo = 9.62 ± 0.01 cc/mol and $K_o$ = 65.0 ± 0.6 GPa for the A7 phase and , Vo = 9.23 ± 0.01 cc/mol and $K_o$ = 72.5 ± 0.3 GPa for the simple cubic phase.

PACS numbers: Phase transitions, crystallographic aspects of, 61.50.Ks

High-pressure effects, structural properties of materials, 81.40.Vw

X-ray diffraction in crystal structure, 61.05.cp

## I. INTRODUCTION

Elemental phosphorus exists as at least three allotropes at ambient conditions including white, black, and amorphous red [1]. Additional allotropes such as crystalline red, gray, violet, and brown, have been made under non-ambient conditions and scarlet, which forms from white when exposed to x-ray radiation. Of these white phosphorus (wP) is the most reactive; igniting in the presence of oxygen. It is widely used in munitions designed for signaling, screening and incendiary purposes. It is also used in the production of phosphoric acid, fertilizers, food additives and cleaning compounds and small amounts are used in pesticides and fireworks. White phosphorus exists as the α form at ambient conditions. It consists of $P_4$ tetrahedra arranged in the body centered cubic α-manganese structure with reported lattice parameters of 18.8Å [2] and 18.51Å [3]. When wP was subjected to high pressure a discontinuous change in volume was observed at 0.8GPa [4] which was interpreted as due to a phase transition to a new phase of wP. The transition pressure was found to fall on decreasing temperature [4]. These experiments reported by Bridgman involved compressing wP to a set pressure, cooling the sample to the temperature of liquid air (-185.7$^o$C) and then allowing the sample to warm. The transition was shown as an arrest in the regular rise in temperature with time [4]. This study gave a transition temperature of approximately -80$^o$C at ambient pressure. An NMR study of wP found that cooling at ambient pressure to -165$^o$C resulted in a transformation to the $\gamma$ phase [5]. On heating, a $\gamma$ phase wP sample was found to transform to the $\beta$ phase at -115$^o$C and then to the $\alpha$ phase at -77$^o$C. An x-ray study by Simon et al. (1987) [6] found the $\beta$ to $\alpha$ transition to be at -76.4$^o$C. A later study by Simon et al. (1997) [7] found the beta to $\alpha$ transition occurred at -76.5$^o$C and the $\gamma$ to beta transition occurred at -175$^o$C using differential thermal analysis and, from x-ray diffraction results, the $\alpha$ to $\beta$ transition occurred at about -80$^o$C and the $\gamma$ to $\beta$ transition occurred at nearly -105$^o$C. A Raman study [8] found the $\beta$ to $\alpha$ transition to occur at -78$^o$C and the $\gamma$ to $\beta$ transition to transpire at -183°C. In all these studies, temperature dependent phase transitions on warming were initiated from the $\gamma$ phase. The $\beta$ phase has been found to have a triclinic structure analogous to that of $\gamma$-plutonium [6]. The structure of the $\gamma$ phase was determined to be monoclinic but close to orthorhombic [9]. The $P_4$ tetrahedra in both the alpha and beta structures show librational disorder[5] while the arrangement in the $\gamma$ phase is virtually static [9]. Both of the low temperature transitions were found to be sluggish.

X-ray studies of wP are difficult due to the material partially transforming to scarlet phosphorus when exposed to x-rays [10]. Perhaps for this reason no measurement of the compressibility of either the alpha or beta forms of white phosphorus has been reported using x-ray radiation. Here we present an x-ray study of the compressibility of white phosphorus and subsequent black phosphorus phases at ambient temperature.

## II. EXPERIMENTAL

White phosphorus, in stick form, was obtained from Thomas Baker (Chemicals) PVT, LTD. and cut under water to achieve approximately 50 micron dimensions and then loaded with a pressure manometer into a diamond anvil cell (DAC) and pressurized in a hydrostatic medium consisting of 16:4:1 ratio of methanol:ethanol:water. Using an analytically calibrated confocal micro-Raman spectroscopy system it was verified that no impurities (e.g., phosphoric acid) were present above the 10 ppm concentration level. The 220 μm diameter by 70 μm tall sample chamber consisted of two counter opposed type Ia 400 μm diameter culet diamonds and a rhenium gasket used to laterally confine samples. Pressure manometers consisted either of ruby [11] or NaCl. Pressure was determined before and after each x-ray measurement and the average is reported. The ruby scale has an error in the pressure of ±5%. When determining pressure using the ruby manometer, the 488nm excitation laser fluence and exposure time were minimized in order to inhibit photo-conversion to grey phosphorus. Data were collected on beamline 12.2.2 at the Advanced Light Source [12,13]. This beamline is equipped with a set of brightness preserving optics that delivers about $2 \times 10^{10}$ photons per second into a 10μm focal spot. An x-ray energy of 25keV was used. A MAR345 imaging plate detector was used to collect diffracted x-rays. We limited the exposure of the sample to x-rays to 60 seconds in order to minimize conversion of the white phosphorus to scarlet phosphorus. A sample was reloaded whenever any sign of conversion to scarlet phosphorus was detected. Approximately ten exposures could be collected using 25keV radiation before any significant coloration of the sample or development of amorphous-like scattering background was observed. Data were collected up to a pressure of 22.4GPa. Two dimensional diffraction patterns were radially integrated using the fit2d program [14]. The sample to detector distance was determined using the $LaB_6$ standard. Peak positions were determined either by whole pattern fitting using the GSAS package [15,16] or by fitting individual peaks with a pseudo-Voigt function. Molar volumes were calculated from the lattice parameters and used to determine values for zero pressure volume and bulk modulus using the third order Birch-Murnaghan equation of state [17].

$$P = \frac{3}{2}K_o\left[\left(\frac{V}{V_o}\right)^{-\frac{7}{3}} - \left(\frac{V}{V_o}\right)^{-\frac{5}{3}}\right]\left[1+\frac{3}{4}(K_o^{'}-4)\left(\left(\frac{V}{V_o}\right)^{-\frac{2}{3}}-1\right)\right]$$

Where P is the pressure, V is the volume at pressure P, Vo is the volume at ambient pressure, $K_o$ is the bulk modulus at ambient pressure and $K_o{'}$ is the pressure derivative of $K_o$. This equation can be written in terms of the strain f:

$$f = 0.5\left[\left(\frac{V}{V_o}\right)^{-\frac{2}{3}}-1\right]$$

and normalized pressure F:

$$F = \frac{P}{1.5\left[\left(\frac{V}{V_o}\right)^{-\frac{7}{3}} - \left(\frac{V}{V_o}\right)^{-\frac{5}{3}}\right]}$$

and rewritten in the form:

$$F(f) = K_o(1 - 2\xi f)$$

where $\xi = \frac{3}{4}(4 - K'_o)$, which can be determined from a plot of F vs f. If the ambient pressure volume is not known then these equations can be rewritten in terms of a nominal ambient volume V* where:

$$g = 0.5\left[\left(\frac{V^*}{V_o}\right)^{-\frac{2}{3}} - 1\right] \quad \text{and} \quad G = \frac{P}{3(1+2g)^{3/2}}$$

and a plot of g versus G gives the ambient pressure which can then be used in a f versus F plot. Molar volumes were calculated for the α phase assuming 232 phosphorus atoms per unit cell [6].

## III. THE STABILITY AND EQUATIONS OF STATE OF WHITE PHOSPHORUS

Hydrostatically compressed white phosphorus was found to remain in the body centered cubic phase up to 2.3GPa (FIG. 1) when it transformed to orthorhombic black phosphorus. Unit cell parameters and molar volumes are listed in table 1. No sign of the triclinic β phase was detected in this pressure range. Close examination of the data revealed a small discontinuity between 0.83 and 0.91GPa which we attribute to the transition observed by Bridgman [4]. Since the x-ray diffraction patterns clearly show no indication of the beta phase of white phosphorus we will refer to it as the α' phase. Taking the mid point of these two pressure points gives a transition pressure of 0.87 ± 0.04 GPa compared to a value of about 0.8 GPa previously observed [4]. A plot of normalized stress as a function of strain (an Ff analysis) [18] was used to determine the bulk modulus and the pressure derivative of the bulk modulus for all data collected below 0.87 GPa. An analysis of the contributions to the calculated pressure from the various orders of strain in the Birch-Murnaghan equation revealed that only the second order term is significant in the pressure stability range of white phosphorus [18]. Consequently only a second order equation was fit to the data. A bulk modulus of 6.7(5) GPa was found for the α phase (FIG. 2). Since no ambient pressure volume exists for the α' phase we have to first determine the ambient pressure volume from a plot of normalized stress as a function of effective strain (a Gg plot) [18] (FIG. 2). A plot of normalized stress as a function of strain was then used to determine the bulk modulus (FIG. 2.). An ambient pressure volume of 16.4 ± 0.1 cc/mol and a bulk modulus of 9.1 ± 0.3 GPa was found. Thus the transition at 0.87 GPa is accompanied by a 36% decrease in compressibility. A gG analysis was also carried out for the α phase data, which gave a value for the ambient pressure volume of 16.94 ± 0.08 cc/mol. This compares well with the literature values of 16.99 cc/mol [3] and 17.02 cc/mol [19] and hence was used in our Ff analysis to compute the bulk modulus and as our initial estimate for the volume in our gG analysis. The ambient pressure volume that we determined gives an ambient pressure lattice parameter for the α phase of 18.68 ± 0.09 Å.

## IV. THE STABILITY AND EQUATIONS OF STATE OF BLACK PHOSPHORUS

The α' phase of white phosphorus transformed into the orthorhombic A17 phase of black phosphorus (bP) at 2.68 ± 0.34 GPa. We further compressed the sample to a maximum pressure of 22.4 GPa. The sample converted from the orthorhombic to the rhombohedral (A7) and then the simple cubic (sc) phase of as expected from previous studies of pure black phosphorus [20,21]. On depressurization the sample was found to transform from the sc to the A7 and then, at about 2.1 GPa, to the A17 phase and to remain in the A17 phase at ambient pressure. Values for lattice parameters and molar volumes are contained in table 1.

Figure 4 contains a comparison of our A17 phase molar volumes with those of Kikegawa and Iwasaki [20]. A two-dimensional Kolmogorov-Smirnov probability distribution test [21,22] was used to quantify the numerical relation between these two sets of data. The K-S formalism sets a confidence level criterion of 0.01 to delineate real correspondence between separate data –a value above 0.01 indicates that unrelated sets of data may be combined to yield a more comprehensive and robust analysis. To carry out this test we implemented the procedures described in Numerical Recipes [23] in Matlab (1984-2010 The MathWorks, Inc.) with a correction to ensure the correct counting of the quadrature point [24]. This gave a K-S statistic of 0.4 with a confidence level 0.56. The confidence level is well above the value of 0.01 required to prove a null hypothesis: the two datasets are not related to each other and it is valid to combine them together. We used Gg and Ff plots to refine the ambient pressure volume, bulk modulus, and the pressure derivative of the bulk modulus using this combined dataset. Only the second order term was found to be significant in the pressure stability range of orthorhombic black phosphorus. We determined a zero pressure volume ($V_o$) of 11.43 ± 0.05 cc/mol and a bulk modulus ($K_o$) of 34.7 ± 0.5 GPa for this combined dataset. Our data points at 2.58 GPa, on compression, and 2.10 GPa on decompression seem to deviate (< 2%) from the general compressional trend developed by Kikegawa and Iwasaki however our measured values fall within their error bars and the Kolmogorov-Smirnov test indicates that the two datasets are drawn from the same distribution so there is no statistic difference between their results and ours.

A comparison of our data for rhombohedral black phosphorus and that of Kikegawa and Iwasaki [18] is illustrated in figure 5. We used the Kolmogorov-Smirnov test to compare these two datasets and determined a K-S statistic of 0.33 with a confidence level of 0.72. Since the confidence level is well above the value of 0.01 needed to prove the null hypothesis we are able to combine these datasets together. We used this combined dataset to determine a zero pressure volume, bulk modulus and pressure derivative of the bulk modulus as above. A second order Birch-Murnaghan equation was found to be sufficient to fit these data. We determined $V_o = 9.62 \pm 0.01$ cc/mol and $K_o = 65.0 \pm 0.6$ GPa for this combined dataset.

We collected three data points in the simple cubic phase. These are compared with the data of Kikegawa and Iwasaki [20] and Akahama et al. [25] in Figure 6. We used the Kolmogorov-Smirnov test to compare these three datasets with each other. Comparison of the Kikegawa and Iwasaki [20] dataset with the Akahama et al. [25] dataset gave a K-S statistic of 0.43 with a confidence level of 0.65. Comparison of the Kikegawa and Iwasaki [20] dataset with our data gave a K-S statistic of 0.25 with a confidence level of 0.99. Comparison of the dataset of Akahama et al. [25] with our data gave a K-S statistic of 0.67 with a confidence level of 0.52. Since these confidence levels are all well above 0.01 it is appropriate to combine these datasets together. A second order Birch-Murnaghan equation was found to be sufficient to fit these data. We determined $V_o = 9.23 \pm 0.01$ cc/mol and $K_o = 72.5 \pm 0.3$ GPa for this combined dataset.

## V. CONCLUSIONS

White phosphorus was found to transform from the initial body centered cubic α form to a less compressible body centered cubic form, called the α' form, at 0.87 ± 0.04 GPa with a 3.5% reduction of molar volume. This transformation occurred at approximately the same pressure as that observed by Bridgman but interestingly it does not correspond to the α to β transition observed at -76.9 $^{o}$C and thought to extend with increasing pressure and temperature to 1.2 GPa and 64.4 $^{o}$C [4]. The α' phase is seen to have a smaller zero pressure volume and larger bulk modulus, or incompressibility, than the α phase which we would expect. White phosphorus transformed into orthorhombic black phosphorus at 2.68 ± 0.34 GPa and then transformed into rhombohedral and simple cubic black phosphorus with increasing pressure as expected from previous work [20,25]. On decreasing pressure the sample remained as black phosphorus transforming from simple cubic to rhombohedral and then orthorhombic in which form it remained to ambient pressure. Our cubic white phosphorus and orthorhombic, rhombohedra and simple cubic black phosphorus volume data were used to determine ambient pressure volumes and bulk moduli. As might be expected the ambient pressure volumes were found to decrease and the bulk moduli were found to increase with increasing pressure of formation for each phase.

## ACKNOWLEDGEMENTS

We thank Martin Kunz and the ALS staff for support on beamline 12.2.2 and the input of an anonymous reviewer which greatly improved this manuscript. JMZ acknowledges partial financial support from the Defense Threat Reduction Agency including the LLNL DOE Campaign II program directed by Dr Kimberly Budil. This work was performed under the auspices of the U.S. Department of Energy by Lawrence Livermore National Laboratory under Contract DE-AC52-07NA27344. The Advanced Light Source is supported by the Director, Office of Science, Office of Basic Energy Sciences, of the U.S. Department of Energy under Contract No. DE-AC02-05CH11231.

[1] S. Bocker and M. Haser, Z. Anorg.allg. Chem. **621,** 258 (1995).

[2] T. Sugawara and E. Kanda, *Science Reports of the Research Institutes Tohoku University* **1**, 153 (1949).

[3] D.E.C. Corbridge and E.J. Lowe, *Nature* **170,** 629 (1952).

[4] P. W. Bridgman, *Phys. Rev.* **3**, 1344 (1914).

[5] H. W. Spiess, R.Grosescu and U. Haeberlen, *Chem. Phys.* **6**, 226 (1974).

[6] A. Simon, H. Borrmann and H. Craubner, *Phosphorus and Sulfur* **30**, 507 (1987).

[7] A. Simon, H. Borrmann and J. Horakh, *Chem. Ber./Recueil* **130**, 1235 (1997).

[8] H. Ostmark, S. Wallin, N. Hore and O. Launila, *J. Chem. Phys.* **119,** 5918 (2003).

[9] H. Okudera, R. E. Dinnebier and A. Simon, *Zeitschrift fur Kristallographie* **220**, 259 (2005).

[10] G. Natta and L. Passerini, *Nature* **125**, 707 (1930).

[11] H. K. Mao, J. Xu and P.M. Bell, J. Geophys. Res., **B91,** 4673 (1986).

[12] M. Kunz, A. A. MacDowell, W. A. Caldwell, D. Cambie, R.S. Celestre, E.E. Domning, R. M. Duarte, A.E. Gleason, J.M. Glossinger, N. Kelez, D.W. Plate, T. Yu, J. M. Zaug, H. A. Padmore, R. Jeanloz, A. P. Alivisatos, and S. M. Clark, *J. Synch. Rad.* **12** 650 (2005).

[13] W. A. Caldwell, M. Kunz, R. S. Celestre, E. E. Domning, M. J. Walter, D. Walker, J. Glossinger, A.A. MacDowell, H.A. Padmore, R. Jeanloz and S.M. Clark, *Nuclear Instrumentation and Methods in Physics Research, Section* A **582,** 221 (2007).

[14] A. P. Hammersley, S. O. Svensson, M. Hanfland, A. N. Fitch and D. Hausermann, *High Pressure Research* **14**, 235 (1996).

[15] B. H. Toby, *J. Appl. Cryst.* **34**, 210 (2001).

[16] A. C. Larson and R.B. Von Dreele, "General Structure Analysis System (GSAS)", *Los Alamos National Laboratory Report LAUR* 86 (2000).

[17] F. Birch, *J. Geophys. Res*. **83**, 1257 (1978).

[18] R. Jeanloz, *Geophysical Research Letters* **8,** 1219 (1981).

[19] J.A. Dean, Lange's Handbook of Chemistry 14th Edition (1992).

[20] T. Kikegawa and H. Iwasaki, *Acta Cryst*. **B39**, 158 (1983).

[21] J.A. Peacock, *Mon. Not. R. Astron. Soc.* **202**, 615 (1983).

[22] E. Gosset, *Astronomy and Astrophysics*, **188**, 258 (1987).

[23] W.H. Press, S.A. Teukolsky, W.T. Vetterling and B.P. Flannery, **Numerical Recipes in C: The Art of Scientific Computing,** Cambridge University Press, Cambridge (1996).

[24] S.A. Metchev and J.E. Grindlay, *Mon. Not. R. Astron. Soc.* **335**, 73 (2002).

[25] Y. Akahama, M. Kobayashi and H. Kawamura, *Phys. Rev. B*, **59**, 8520 (1999).

[26] K. Patz *Zeitschrift fur Anorganische und Allgemeine Chemie* **285**, 29 (1956).

[27] R. B. Jacobs, *J. Chem. Phys.* **5**, 945 (1937).

[28] I. Shirotani, et al., *Phys. Lett. A* **144**, 102 (1990).

| **Phase** | **Pressure (GPa)** | **a(Å)** | **b(Å)** | **c(Å)** | **Molar volume (cc/mol)** |
|---|---|---|---|---|---|
| α-wp | 0.06(10) | 18.642(9) | | | 16.816(8) |
| α-wp | 0.14(10) | 18.559(9) | | | 16.593(8) |
| α-wp | 0.13(10) | 18.548(9) | | | 16.563(8) |
| α-wp | 0.31(10) | 18.421(9) | | | 16.225(8) |
| α-wp | 0.52(10) | 18.255(9) | | | 15.791(8) |
| α-wp | 0.72(10) | 18.147(9) | | | 15.512(8) |
| α-wp | 0.83(10) | 18.088(9) | | | 15.361(8) |
| α’-wp | 0.91(10) | 18.021(9) | | | 15.191(8) |
| α’-wp | 0.98(10) | 17.966(9) | | | 15.052(7) |
| α’-wp | 1.17(10) | 17.862(9) | | | 14.793(7) |
| α’-wp | 1.19(10) | 17.860(9) | | | 14.788(7) |
| α’-wp | 1.21(10) | 17.832(9) | | | 14.718(7) |
| α’-wp | 1.66(8) | 17.670(9) | | | 14.321(7) |
| α’-wp | 1.81(9) | 17.630(9) | | | 14.224(7) |
| α’-wp | 2.23(11) | 17.424(9) | | | 13.731(7) |
| o-bp | 2.58(12) | 3.302(7) | 9.94(2) | 4.22(1) | 10.43(7) |
| o-bp | 3.8(1) | 3.299(4) | 9.935(9) | 4.206(5) | 10.38(3) |
| o-bp | 4.1(1) | 3.302(3) | 9.919(6) | 4.206(4) | 10.37(3) |
| o-bp | 4.5(1) | 3.301(5) | 9.922(9) | 4.192(4) | 10.34(3) |
| h-bp | 7.3(3) | 3.388(7) | | 8.669(2) | 8.65(3) |
| h-bp | 10.0(1) | 3.374(9) | | 8.604(3) | 8.51(4) |
| sc-bp | 13.6(3) | 2.375(2) | | | 8.067(7) |
| sc-bp | 17(1) | 2.346(4) | | | 7.78(1) |
| sc-bp | 22.4(8) | 2.321(2) | | | 7.531(5) |
| h-bp | 9.44(10) | 3.393(9) | | 8.669(2) | 8.67(4) |
| h-bp | 7.5(1) | 3.389(2) | | 8.709(1) | 8.69(1) |
| h-bp | 5.37(10) | 3.414(3) | | 8.810(2) | 8.93(2) |
| h-bp | 4.6(1) | 3.420(3) | | 8.857(1) | 9.00(1) |
| h-bp | 4.23(10) | 3.423(3) | | 8.887(1) | 9.05(1) |
| h-bp | 3.1(1) | 3.434(5) | | 9.010(2) | 9.24(3) |
| h-bp | 3.0(1) | 3.434(3) | | 9.010(2) | 9.24(2) |
| o-bp | 2.1(3) | 3.29(1) | 10.11(2) | 4.20(2) | 10.5(1) |
| o-bp | 0.0(3) | 3.310(2) | 10.479(1) | 4.387(5) | 11.45(2) |

**Table I. Lattice parameters and molar volumes determined for white phosphorus (wp) and subsequent black phosphorous (bp) phases. o-bp the orthorhombic phase of black phosphorus, h-bp the hexagonal phase of black phosphorus and sc-bp the simple cubic phase of black phosphorus.**

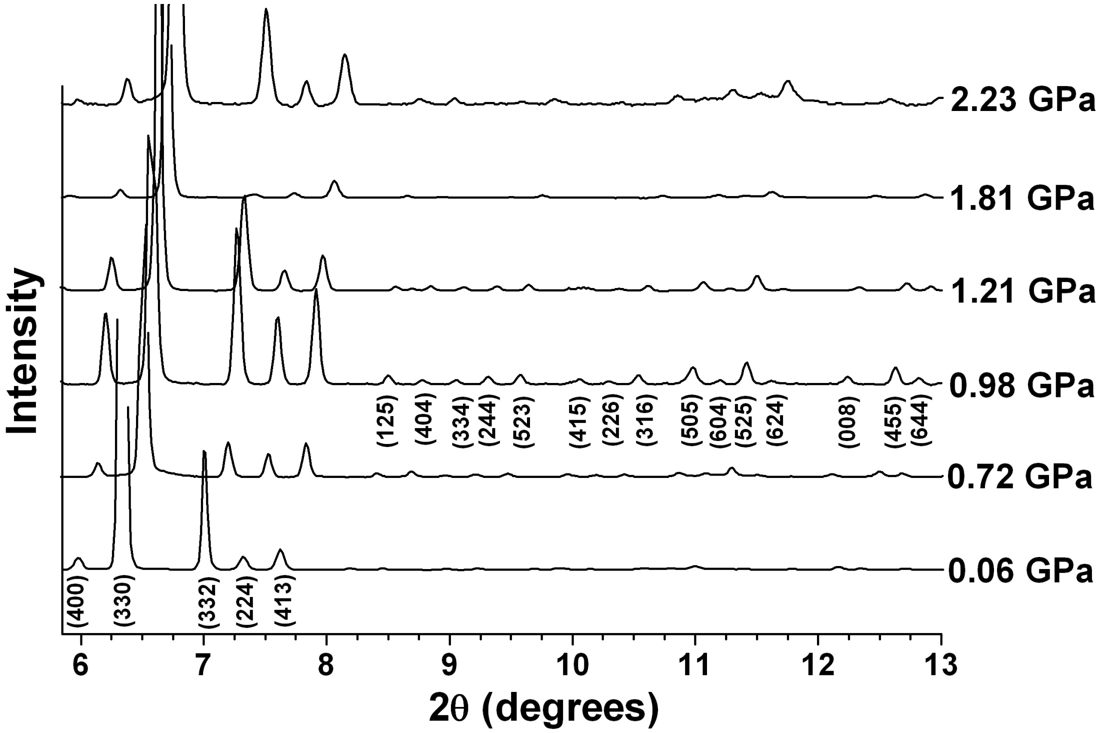

**FIG. 1. Plot of six diffraction patterns of white phosphorus taken from ambient to just below the phase transition to orthorhombic black phosphorus. All of the available data were not plotted to increase clarity. The miller indices for the strongest peaks are included.**

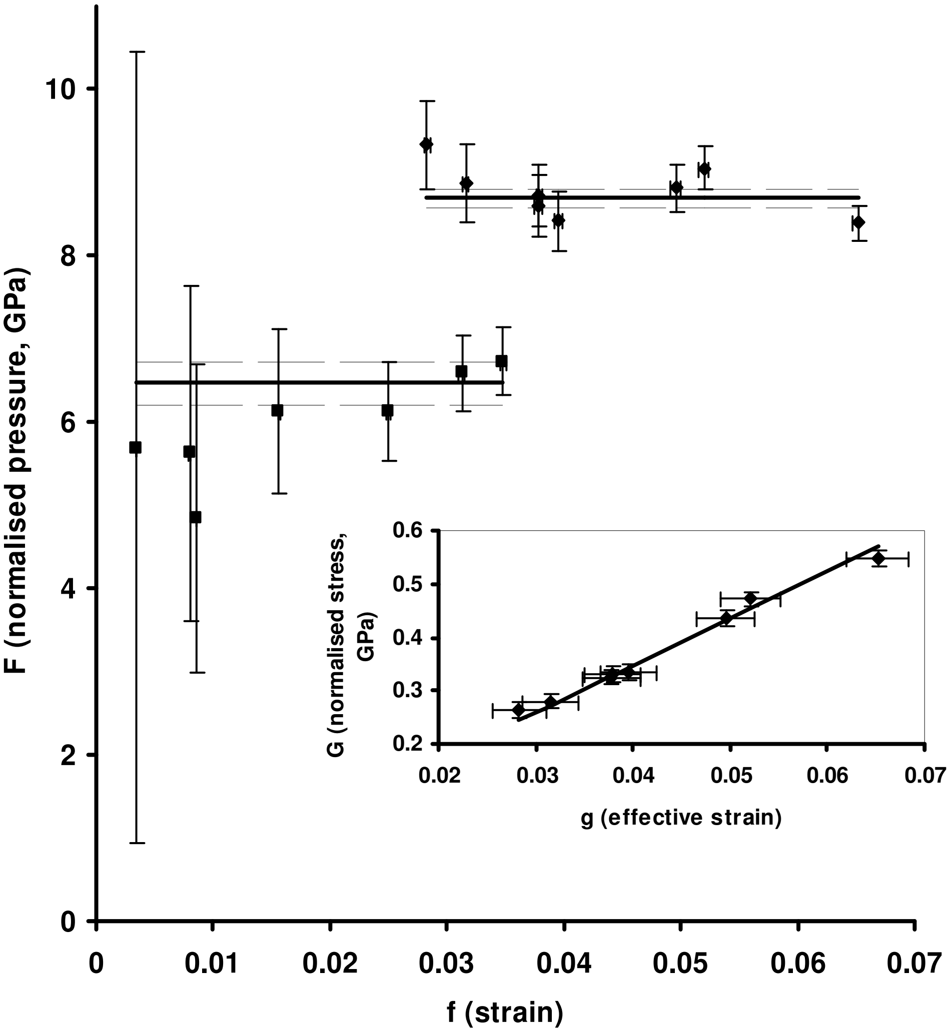

FIG. 2. The main figure shows plots of strain against normalized pressure for the α and α' phases of white phosphorus. The insert shows the g versus G plot used to determine the ambient volume of the high pressure phase.

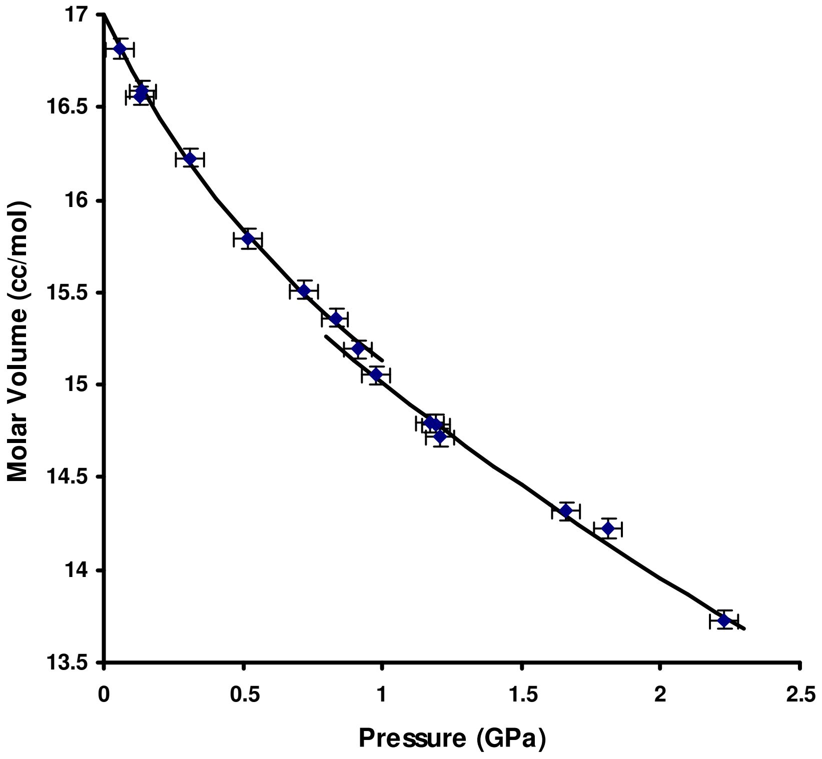

**FIG. 3.** The molar volume of white phosphorus as a function of pressure at ambient temperature. The diamonds are the measured data points and the lines are fits to the second order Birch-Murnaghan equation using the data above and below 0.87 GPa.

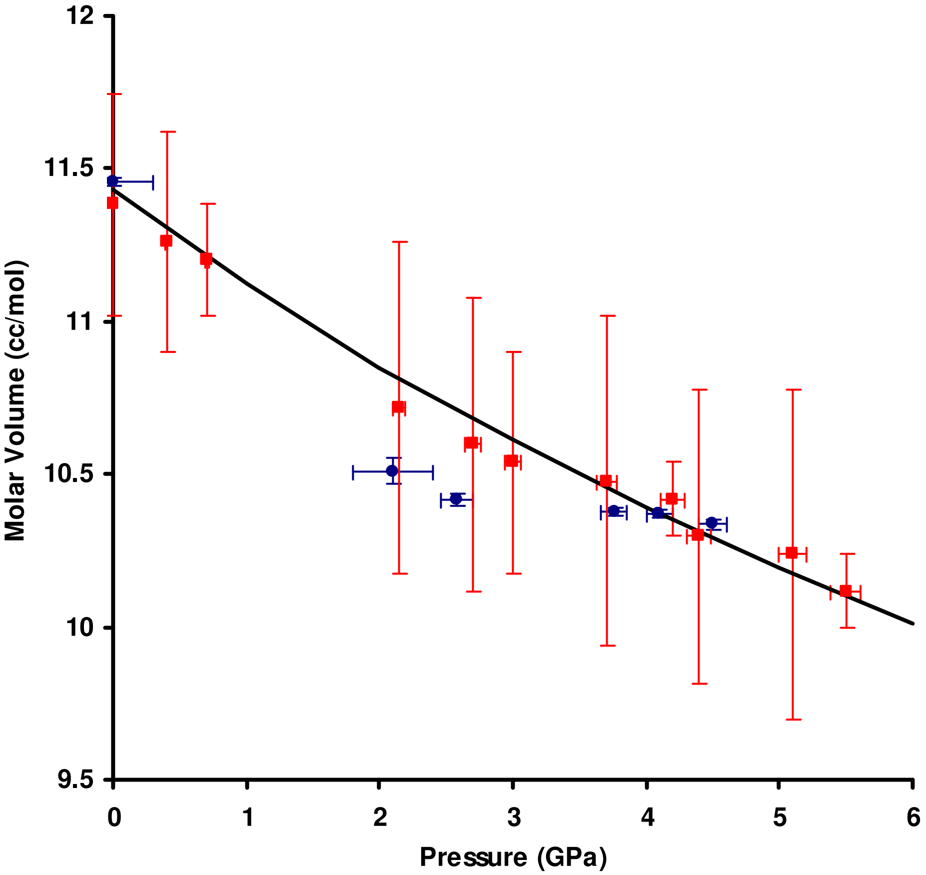

FIG. 4. The volume of the orthorhombic form of black phosphorus as a function of pressure at ambient temperature. Our data are shown as filled blue circles and the data of Kikegawa and Iwasaki [20] are shown as filled red squares. Our datum at ambient pressure is from recovered material after compression. A fit to the second order Birch-Murnaghan equation using all of the data is shown as a solid black line.

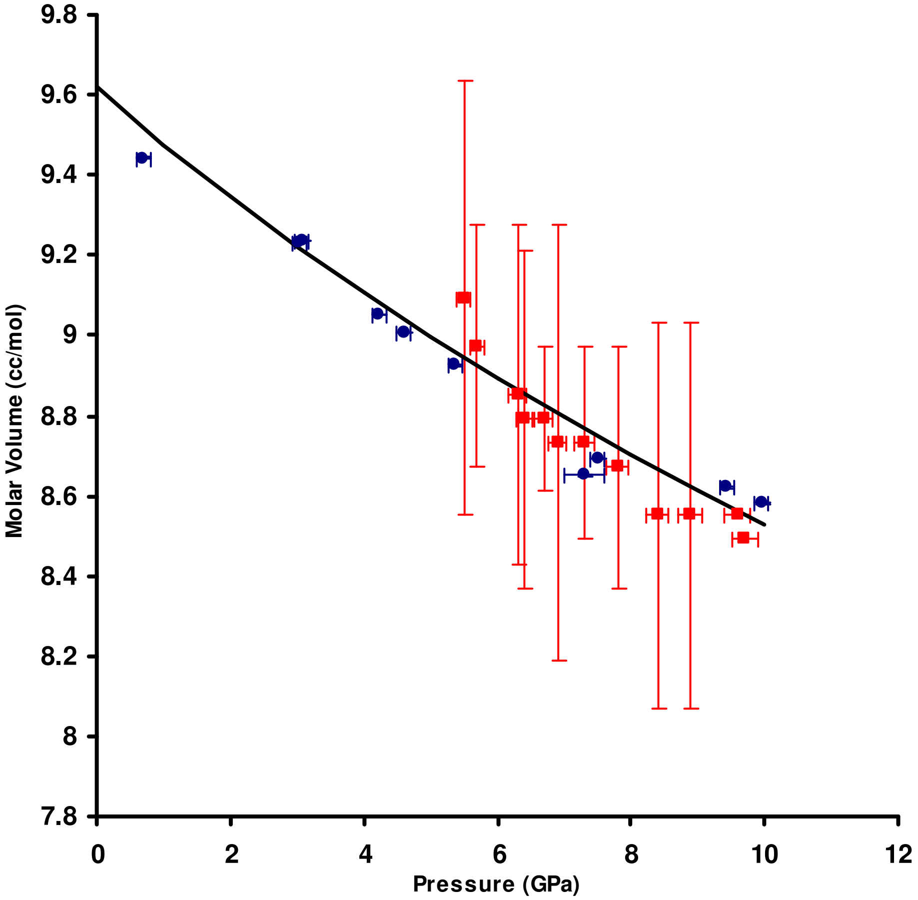

FIG. 5. The volume of the rhombohedral form of black phosphorus as a function of pressure at ambient temperature. Our data are shown as filled blue circles and the data of Kikegawa and Iwasaki [20] are shown as filled red squares. Our lowest pressure datum was measured during the decompression cycle of the experiment. A fit to the second order Birch-Murnaghan equation using all of the data is shown as a solid black line.

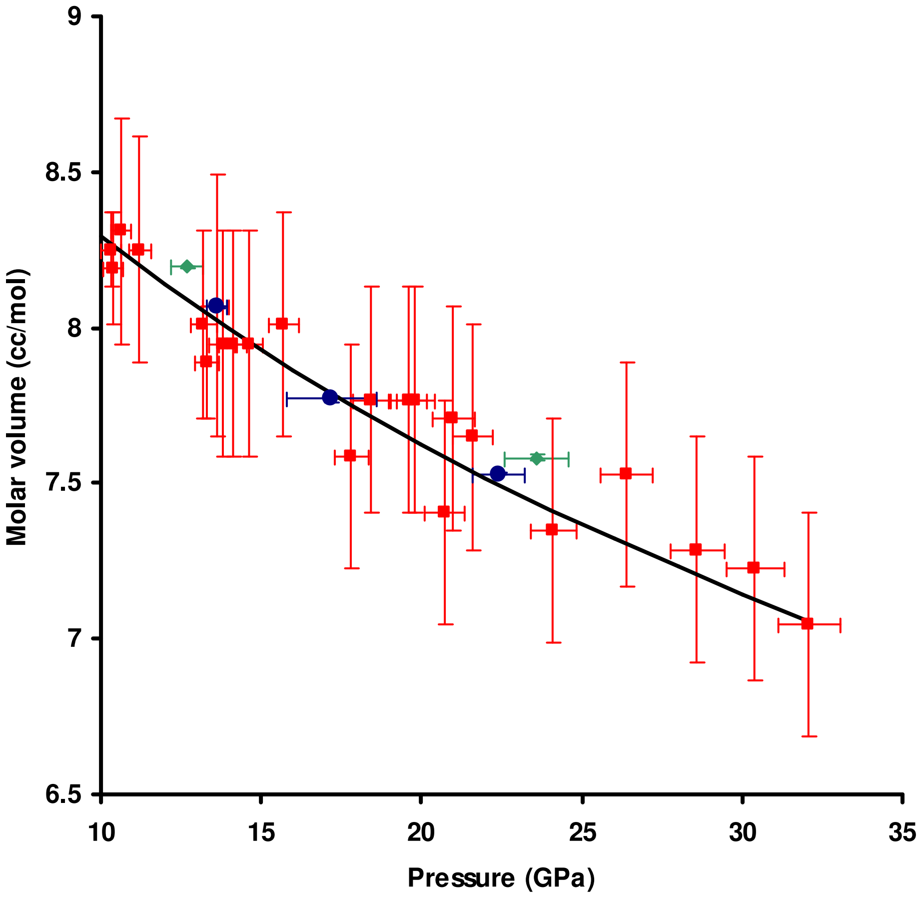

FIG. 6. The volume of the simple cubic form of black phosphorus as a function of pressure at ambient temperature. Our three data points are shown as filled blue circles, the data of Kikegawa and Iwasaki [20] are shown as filled red squares, and the data of Akahama et al. [25] are shown as filled green diamonds. A fit of a third order Birch-Murnaghan equation to all of this data is shown as a solid black line.

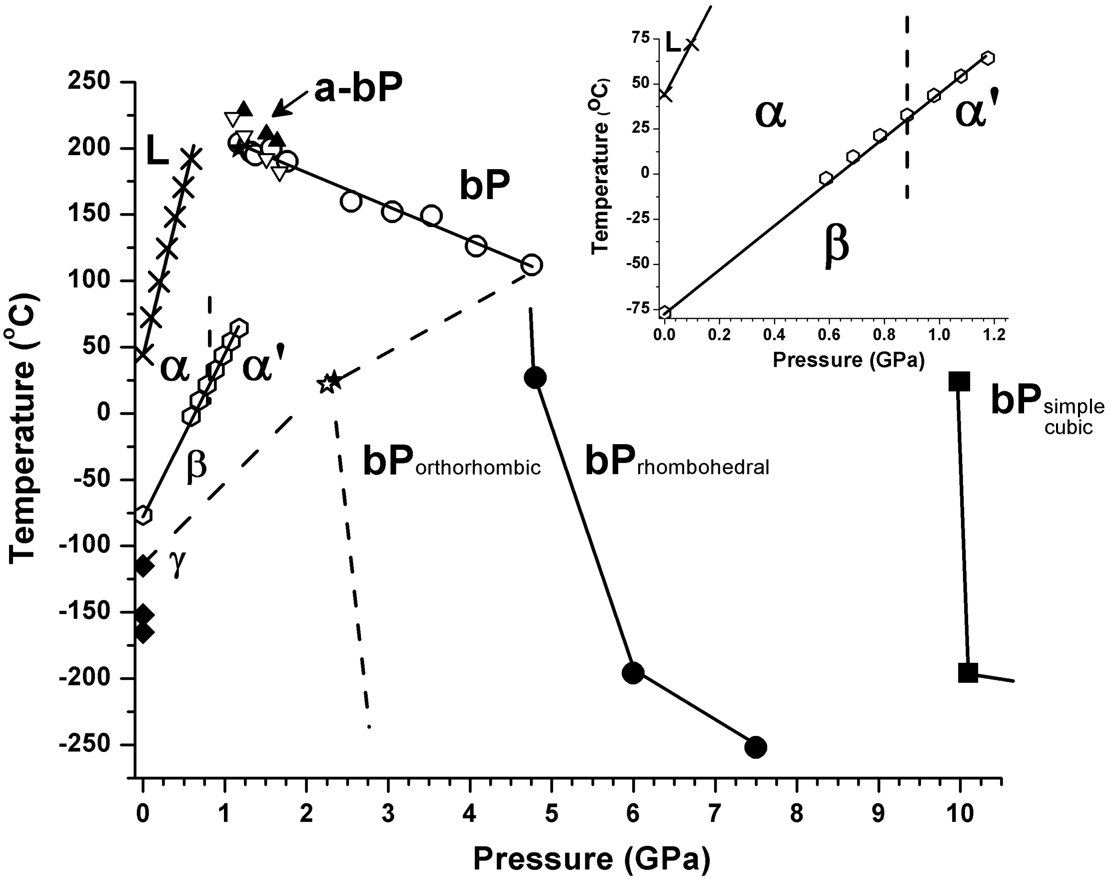

FIG. 7. The metastable phase diagram for white phosphorus. The white allotrope stability field consists of the γ phase, solid diamonds at ambient pressure by Simon et al. [7] and Okudera et al. [9]; the β - α phase boundary, open hexagons by Bridgman [4] (using the originally reported pressure values); the α - α' phase boundary at ambient temperature, dashed vertical line at 0.87 GPa (see inset), this work; the solid alpha-liquid transition line, crosses by Bridgman [4]; the α –black phosphorus (bP) transitions, open circles by Patz [26], open downward triangles to amorphous black phosphorus (a-bP) (70 min. conversion

**time) and solid upward triangles to a-bP (10 min. conversion time) by Jacobs [27], black stars to a-bP and bP orthorhombic phases by Bridgman [4], α'-bP orthorhombic, open white star this work; the γ white-bP orthorhombic dashed transition line is drawn only as a suggestion; the bP orthorhombic-bP rhombohedral transition line, solid circles by Shirotani et al, [28]; and the bP rhombohedral-bP simple cubic transition line by Kikegawa [20].**